File ID    363234
Filename    Chapter 3: Size exclusion chromatography × reversed phase liquid chromatography for the analysis of complex peptide mixtures

SOURCE (OR PART OF THE FOLLOWING SOURCE):
Type    Dissertation
Title    Modes of operation and parameter selection in on-line comprehensive two-dimensional liquid chromatography
Author    F. Bedani
Faculty    Faculty of Science
Year    2012
Pages    viii, 124

FULL BIBLIOGRAPHIC DETAILS:
    http://dare.uva.nl/record/417576

# Chapter 3

# A theoretical basis for parameter selection and instrument design in comprehensive size-exclusion chromatography × liquid chromatography

## Abstract

*A novel approach for the selection of the operational parameters (linear velocity, column length) for an on-line comprehensive two-dimensional liquid chromatography (2D-LC) system is discussed. Starting point for the calculations is a given second-dimension separation and a desired peak capacity for the 2D system. Using the theory developed here the optimum settings for the first-dimension column can be derived. Theory clearly indicates that the choice of the first-dimension conditions is basically limited to just one set of column lengths and linear velocities. The new method is tested on an on-line comprehensive 2D-LC system which uses size exclusion chromatography (SEC) followed by reversed phase liquid chromatography (RPLC). A novel 2D-LC interface, using a six-port valve rather than storage loops, joins the two chromatographic dimensions. From a theoretical comparison of continuous low-flow and stop-flow operation the latter method was found to be an attractive mode of interfacing. The common idea that stop-flow operation results in additional band broadening is shown to be incorrect. The new interface design operated in the stop-flow mode permits the use of conventional analytical diameter HPLC columns, 7.8 mm for SEC and 4.6 mm for RPLC. The reversed phase chromatography utilizes a monolithic C18 modified silica column, which produces fast and efficient analyses. As test samples complex mixtures of peptides were analyzed.[1]*

---

# Contents

## 3.1 Introduction

It has long been known that "complex samples require analytical methods of extremely high resolving power in order to provide reliable analyses of the sample components" [1]. In LC, one well established way to enhance resolving power, is to carry out analyses in more than one analytical dimension. Protein hydrolysates are a clear example of complex samples. One of the most commonly used techniques for peptide analysis in such samples is reversed phase liquid chromatography (RPLC) coupled to mass spectrometry (MS) [e.g. 2-4]. While, for such systems, it is easy for the mass spectrometer to identify the presence of a few coeluting peaks, data interpretation becomes difficult if a large number of peptides coelute. To circumvent this problem, comprehensive two-dimensional liquid chromatography (LC × LC, following the notation of Schoenmakers et al. [5]) can be utilized [1, 6-9].

Comprehensive 2D-LC techniques differ from ordinary heart-cutting 2D-LC ones [10-12] in that they subject the entire sample to the separation [13-15]. Both LC × LC and heart-cutting 2D-LC can be performed in two different ways [11]: so called "off-line" operation requires the eluate from the first-dimension ($^1$D) to be collected as narrow fractions and stored. Fractions of interest are subsequently reinjected onto the second dimension column. "On-line" operation means that transfer of effluent fractions from the first- to the second-dimension is executed automatically within the confinement of the 2D-LC system. Then, a rapid separation is performed such that the second-dimension ($^2$D) column is ready to receive the next fraction and perform a new separation. Because of the automated and on-line nature of the system, the operator is much less involved, and the chances for sample handling losses during transfer are eliminated. Further, any partial separation accomplished during the first-dimension is maintained by not recombining the fractions as they are transferred to the second-dimension.

LC × LC offers a substantially higher chromatographic resolution than any one-dimensional (1D) LC technique, because of the unlikelihood of two components having the same retention times in both dimensions. As derived by Giddings [16], LC × LC resolving power is ideally given by the product of the resolving power of the two underlying 1D separations. However, the LC × LC resolving power estimated in this way can only be utilized if two conditions are met: the two *phase systems* (stationary *and* mobile phase combinations) are "fully" orthogonal and the resolving power generated independently by the two columns can be maintained [17].

In LC × LC separations of (bio)polymers several different separation mechanisms can be exploited in the first- and second-dimension. These include e.g. RPLC, SEC, ion exchange chromatography (IEC) and capillary electrophoresis. In this chapter, an on-line LC × LC system where SEC is used as the $^1$D and RP as the $^2$D is exploited. The main reason for using SEC in the $^1$D is the fact that refocusing on top of the $^2$D column in this case is rather easy to obtain. In a recent study conducted on different 2D-LC systems, Gilar et al. [18] have concluded that SEC and RP provide an excellent orthogonality at a reasonable peak capacity.

Evidently, when setting up 2D-LC systems, both the choice of the columns for the two dimensions as well as of the operational parameters is crucial. This has up to now mainly

been performed using trial-and-error strategies, notable exceptions here being works by Schoenmakers et al. [19] and Vivó-Truyols et al. [20]. In order to make the optimization process less empiric, a novel approach is discussed here. This approach is meant to provide chemists entering the area of LC × LC with a strategy resulting in a more straightforward way to optimize the relevant parameters of an LC × LC separation. The main difference between the work presented in this chapter and the approaches followed by Schoenmakers' and Vivó-Truyols' comes from a practical perspective: whereas in the latter case the complete optimization of the 2D system is described as such without any *a priori* boundary conditions, the starting point in our work is an existing 1D-LC separation for which the desire is to improve peak capacity without the need to re-optimize the original separation. This can be done by adding another dimension. Therefore, a new column - the $^1$D column in the new LC × LC system - needs to be added and optimized. This approach nicely reflects the practical situation in laboratories dealing with complex samples: the current separation performance suffices, but if there was a simple way to improve it this could be worthwhile pursuing.

What will finally be shown is that, once one of the columns has been selected, the choice for the other dimension is much more limited than it might be expected at first sight, if optimal separation conditions need to be met. Starting point of the method derived here is the criterion introduced by Murphy et al. that the optimum number of fractions to be transferred from the first- to the second-dimension is in the order of four per peak [21].

Instrumentation is set up for the on-line SEC × LC separation of mixtures of small peptides. In designing the actual interface care was taken to minimize the risk of adsorptive losses of peptides in valves, tubing, loops, etc. In the present chapter, on-line LC × LC is investigated by working in the stop-flow mode. When operating in stop-flow mode, the $^1$D pump is switched off for the time of the $^2$D run and it is switched on again when transferring the next fraction. The consequences of stop-flow operation in terms of band broadening are studied from a theoretical perspective and system performance in stop-flow is compared to operation at a continuous low-flow.

## 3.2 Theory

### 3.2.1 Optimum column dimensions and operational settings

As emphasized in Section 3.1, one of the most interesting aspects of LC × LC is that, if orthogonal separation conditions are used, the peak capacity of LC × LC systems is greatly enhanced in respect with 1D-LC ones. Below we will derive equations to describe the optimal column dimensions and operating conditions for the first-dimension (assuming isocratic operation) starting from a fixed second-dimension separation.

For LC × LC systems, the total peak capacity of the two columns, $n_{c,tot}$, is ideally given by Eq. 3.1 [16]:

$$n_{c,tot} = {}^1n_c \times {}^2n_c \tag{3.1}$$

where ${}^1n_c$ and ${}^2n_c$ represent the peak capacity in the first- and second-dimension, respectively. As stated above, starting point of this exercise is a given 1D-LC separation and a desire to improve the separation quality by converting this 1D-LC system into an LC × LC one. This implies that the separation in the ${}^2$D has already been fixed and that the total desired peak capacity is set.

Starting point for the theory to be derived here is the criterion introduced by Murphy et al. [21] that the optimum number of fractions to be transferred from the first- to the second-dimension in comprehensive chromatography is in the order of four per peak. When this criterion is applied in the strictest sense, the standard deviation of the narrowest peak in the first-dimension (${}^1$D) expressed in units of time, ${}^1\sigma_t$, is related to the total analysis time in the second-dimension, ${}^2t_a$, by means of the following relationship:

$$^1\sigma_t = {}^2t_a \tag{3.2}$$

Here, ${}^2t_a$ is the sum of the analysis *and* the reconditioning time. Eq. 3.2 clearly links the operation of the ${}^1$D column to the performance of the ${}^2$D.

The next step in the theory derived here is the calculation of the required plate number for the ${}^1$D column. From the desired total peak capacity and the known peak capacity for the ${}^2$D, the peak capacity necessary for the ${}^1$D can be determined from Eq. 3.1. Basically

this implies that a certain plate number is needed for the first-dimension. From $^1n_c$ (in isocratic LC), the required plate number (for adjacent peaks at $R_s = 1$) for the $^1$D column, $^1N$, can be calculated by [22]:

$$^1N = \frac{16 \ (\ ^1n_c - 1\ )^2}{(\ln(\ ^1t_{max} /\ ^1t_{min}))^2} \tag{3.3}$$

where $^1t_{max}$ and $^1t_{min}$ are the limits to the time range in which peaks can elute. In SEC the approximation can be made that $t_{max}/t_{min} = 2$. The column length necessary for getting $^1N$, $^1L$, can be easily calculated from:

$$^1L = {}^1N \times {}^1H(u) \tag{3.4}$$

Here $^1H(u)$ represents the plate height of the $^1$D column used. Evidently $^1H(u)$ is a function of $u$ which is defined here as the chromatographic velocity of the peak of interest, i.e. the column length divided by the retention time of the analyte. As known, $^1N$ can also be expressed by:

$$^1N = \frac{^1t_R^2}{^1\sigma_t^2} \tag{3.5}$$

where $^1t_R$ is the peak retention time in the $^1$D. Substitution of Eq. 3.2 into Eq. 3.5 and its further substitution into Eq. 3.4 gives:

$$^1L = {}^1H(u) \times \frac{^1t_R^2}{^2t_a^2} \tag{3.6}$$

The retention time in the $^1$D, $^1t_R$, is related to $^1u$ by:

$$^1t_R = \frac{^1L}{^1u} \tag{3.7}$$

Combination of Eq. 3.6 and Eq. 3.7 gives:

$$^1L = \frac{^2t_a^2 \times ^1u^2}{^1H(u)} \tag{3.8}$$

Eq. 3.8 gives an explicit equation for the column length in the $^1$D. In order to derive an equation for $^1u$, Eq. 3.4 can be substituted into Eq. 3.8. After rearrangement this gives:

$$\frac{^1H(u)}{^1u} = \frac{^2t_a}{\sqrt{^1N}} \tag{3.9}$$

The plate height of the $^1$D column as a function of $^1u$ can be described by the well-known van Deemter equation:

$$^1H = A + \frac{B}{^1u} + C^1u \tag{3.10}$$

Substitution of Eq. 3.10 in Eq. 3.9 and rearranging gives:

$$\left( \frac{^2t_a}{\sqrt{^1N}} - C \right) \times ^1u^2 - A \times ^1u - B = 0 \tag{3.11}$$

Eq. 3.11 is a second order equation where $^1u$ is the unknown. The meaningful solution for $^1u$ is given by:

$$^1u = \frac{A + \sqrt{A^2 - 4\left(\dfrac{^2t_a}{\sqrt{^1N}} - C\right)(-B)}}{2\left(\dfrac{^2t_a}{\sqrt{^1N}} - C\right)}$$ (3.12)

Substitution of the $^1u$ value obtained from Eq. 3.12 into Eq. 3.10 yields $^1H$ and then, from Eq. 3.8, the required value for $^1L$ can be obtained.

The final result of this exercise is surprising. The theory derived here shows that, for one given *H(u)* curve of the $^1$D column, only *one* column length can be used at *one* specific velocity. Neither longer nor shorter columns nor columns operated at other velocities can simultaneously meet the two requirements specified at the start of the theory section of a desired total peak capacity and of four $^2$D runs over a $^1$D peak. Only one set of conditions can be adopted for the $^1$D. All other conditions result in non-optimal comprehensive separations.

A quick look to Eq. 3.11 suggests that there is no physically meaningful solution if $^2t_a/\sqrt{^1N} \leq C$. From the practical perspective this means that the *C*-term of the van Deemter curve of the $^1$D column defines both the lower limit of $^2t_a$ (at a given $^1N$) and the upper limit of $^1N$ (at a given $^2t_a$). If lower values of $^2t_a$ or higher values of $^1N$ need to be obtained, a $^1$D column with a lower *C*-term, i.e. a shorter plate time, must be used.

At this point it is important to emphasize that the theory derived above was derived for SEC × RPLC but is equally valid for other modes of LC × LC. This means that secondary interactions that will be difficult to avoid in aqueous-SEC will not change the main conclusions drawn here.
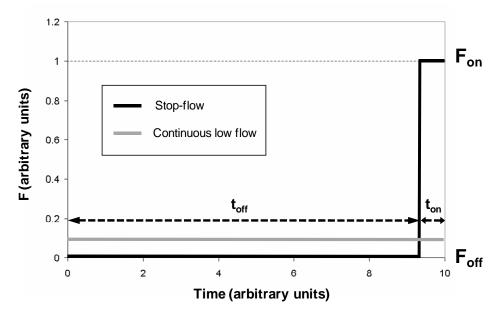
### 3.2.2 Practical consequences

Typical values of $^2t_a$ and $^1N$ with realistic *A*, *B* and *C* values for the van Deemter curve will result in very low $^1u$ values as solutions to Eq. 3.12. Indeed, the first-dimension in practical LC × LC separations is normally operated at low velocities. So far, the way to realize this in all published systems is by running the $^1$D column at a low flow rate. There are, however, basically two ways to obtain low $^1$D velocities: run the system at a

continuous low-flow or use an intermittent high flow - zero flow operation, i.e. stop-flow. In terms of instrument design (see Section 3.4.5), stop-flow operation could be attractive. Below, a comparison in terms of band broadening for the two operational modes is presented. Velocities and on/off times for the stop-flow approach are selected in a way that the average linear velocity is the same as in the continuous low-flow experiment. Below the calculation is performed for one interval i.e. one on/off step or one fraction transferred to the $^2$D. A schematic representation of such an "interval" is given in Figure 3.1. This time period is then repeated *n* times, where *n* is the number of fractions transferred from the first- to the second-dimension.

In the continuous low-flow mode, if a single interval is considered, the total variance in units of length, $\sigma_{z,i}^2$, is given by:

$$\sigma_{z,i}^2(cont) = H(u_{cont}) \times t_i \times u_{cont} \tag{3.13}$$

where $H(u_{cont})$ is the plate height, $t_i$ is the length of the interval and $u_{cont}$ the chromatographic velocity of the peak of interest. The plate height, $H(u_{cont})$, can be calculated by means of Eq. 3.10.



**Figure 3.1**: Flow rate, *F*, for stop-flow and continuous low-flow operation as a function of the interval time.

When referring to the stop-flow mode of operation, in order to estimate the total variance of the band, $\sigma_{tot,z}^2$, the rule of additivity of variances can be used. If a single interval is considered, its variance, $\sigma_{z,i}^2(sf)$, will be given by:

$$\sigma_{z,i}^2(sf) = \sigma_{z,i}^2(cont) + \sigma_{off}^2 \tag{3.14}$$

where $\sigma_{off}^2$ is the variance during stop-flow (in length units). The contribution to the total variance of zero flow operation, $\sigma_{off}^2$, is given by the Einstein diffusion equation:

$$\sigma_{off}^2 = 2D_{eff}t_{off} \tag{3.15}$$

where $t_{off}$ is the stop-flow time and $D_{eff}$ the effective diffusion coefficient of the solute in the column.

## 3.3 Experimental section

A system for comprehensive SEC × RPLC was constructed in-house. The first-dimension used a 7.8 × 300 mm TSK-GEL G2500PW$_{XL}$ column (Tosoh Bioscience, Stuttgart, Germany) packed with 6 μm particles. The mass range of this column, estimated for linear molecules by using polyethylene glycols/oxides (PEG/PEO), is up to 3,000 Da. The second-dimension consisted of a monolithic C18 modified silica 4.6 mm ID × 25 mm long Chromolith Flash column (Merck, Darmstadt, Germany) and a monolithic C18 modified silica 4.6 mm ID × 10 mm long Chromolith Flash Guard column (Merck).

A schematic drawing of the system is shown in Figure 3.2: the SEC column outlet is connected to a six port valve (Valco Instruments, Houston, TX, USA). In the transfer mode the effluent from the $^1$D column is directed to the $^2$D column. The $^2$D gradient pump is now connected to a flow restrictor to keep the pressure constant during the actual transfer. In the $^2$D analysis mode, the $^1$D pump is connected to a stop-flow valve: before the first peak elutes, the stop-flow valve is open, letting the dead volume go to waste. When the transfer of the first fraction starts, the stop-flow valve is switched to the stop-
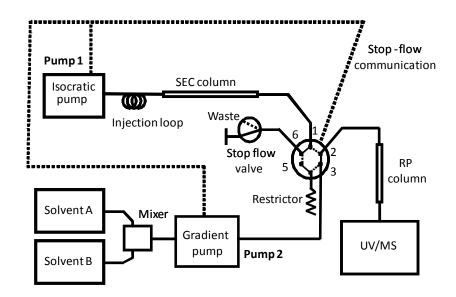
flow position so that, when switching the $^1$D pump off, the pressure in the $^1$D column stays constant. At the end of the analysis the stop-flow valve is switched back to the initial "waste" position.

The mobile phase for the $^1$D column was water (Elgastat Option2 Water Purifier, Salm en Kipp BV, The Netherlands) containing 0.1% trifluoroacetic acid (Sigma-Aldrich Chemie, GmbH, Steinheim, Germany), filtered through a type HVLP 0.45 μm membrane filter (Millipore, Billerica, MA, USA). The separations in the $^1$D column were run either at 0.37 or at 0.50 mLmin$^{-1}$. The mobile phase was supplied by a Model 600 pump (Waters Associates, Milford, MA, USA) and controller. In the $^2$D column, a steep gradient at 2 mLmin$^{-1}$ was pumped by a Model LC-10 AD vp pump (Shimadzu) equipped with a Model FCV-10 AL vp low-pressure mixing chamber (Shimadzu). Mobile phase A was water with 0.1% TFA and B was acetonitrile (Biosolve bv, Valkenswaard, the Netherlands) also containing 0.1% TFA, both passed through a type HVLP 0.45 μm membrane filter. In a typical $^2$D run, a slice of 30 s was transferred at a moderate (0.37 or 0.50 mLmin$^{-1}$) flow rate from the first- to the second-dimension. At the end of the 30 s, the six-port valve was switched and the gradient started. In the next 30 s the initial flow rate was increased to 2 mLmin$^{-1}$ and, after that, the solvent programming started. Flow rate programming was applied to avoid pressure shocks during the actual transfer (the maximum pressure tolerable by the $^1$D column is only 4.3 MPa). A typical gradient started at 5% B; at 2.50 min B was 40% and, at 3.50 min, 90%. B was then maintained at 90% up to 5.50 min and, at 6.50 min, was decreased to 5%. At 7.50 min the percentage of B was 5% and, at 8.50 min, the flow rate was decreased to the starting value.
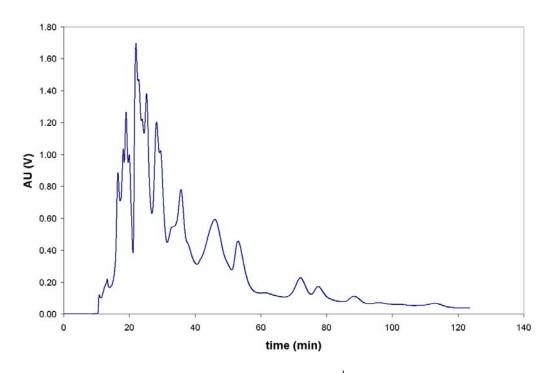
The UV detector (Waters Associates Model 486) monitored absorbance of the peptide bond at 214 nm.

The chromatography system was controlled by Empower software from Waters. The sampling frequency was set at 10 points per second.

Data visualization was performed by Matlab 7.0.1 software, using routines written in-house. For correct visualization data were aligned. We used a signal that appeared at the end of the $^2$D injection as a reference. The alignment was performed in such a way that the corrected retention time of this signal was forced to be constant.

**Figure 3.2**: Schematic representation of the on-line SEC × RPLC system operated in stop-flow mode.



**Figure 3.3:** SEC separation of BioZate3. $F$ = 0.5 mLmin$^{-1}$. Sample concentration: 100 mgmL$^{-1}$. Injection volume: 20 μL. Temperature: 30 °C.

Various complex peptide samples were studied. Most of the work was done using BioZate3, a highly complex whey protein hydrolysate (Davisco Foods, Eden Prairie, MN, USA). BioZate3 contains a high percentage (more than 40%) of low molecular weight peptides (MW < 2000 Da). Previous unpublished work on BioZate3 by LC-MS has

shown that this sample contains thousands of individual peptides. A typical [1]D SEC run for BioZate3 is shown in Figure 3.3.

**3.4 Results and discussion**

*3.4.1 Obtaining input properties H/u and D$_{eff}$*

   The equations derived in earlier sections require accurate *H/u* curves and diffusion coefficients as input parameters. Since such information is hardly available, the required data had to be obtained experimentally. An *H vs u* curve was obtained by running a dipeptide (Ala-Val, MW=198 Da) at different linear velocities on the [1]D-SEC column. The Van Deemter equation was fitted to these experimental data using software written in-house. The *A*-term was found to be $1.5 \times 10^{-5}$ m and the *C*-term $8.6 \times 10^{-2}$ s. The *A*-value is close, for a particle size of 6 μm, to the theoretical minimum of $2d_p$; the *C*-value is reasonable for a low molecular weight analyte. In principle also the *B*-term can be obtained from the experimental *H/u* curve. A reliable estimate, however, is only possible if sufficient data points recorded at very low linear velocities are available. Because this is time-consuming, the *B*-term was calculated from the value of the effective diffusion coefficient, $D_{eff}$. As in Eq. 3.10 the chromatographic velocity is used, *B* is given by $B = 2 \times D_{eff}$. The procedure to obtain $D_{eff}$ from stop-flow experiments was described by Knox [23]. In short, a band of solute was eluted part way through the chromatographic column. The elution was arrested for a constant time, $\Delta t_{off}$, and next the band was eluted at the original flow-rate.

   Two low-MW peptides, Ala-Val (MW=198 Da) and (Ala)$_5$ (MW=373 Da), were used as test compounds. The results are reported in Figure 3.4, where the total variance, $\sigma_t^2$, is plotted against $\Delta t_{off}$.

   The longitudinal variance of the band measured as a length inside the column, $\sigma_z^2$, arising from molecular diffusion in axial direction while a band resides in the column, is given by Eq. 3.16 [23]:
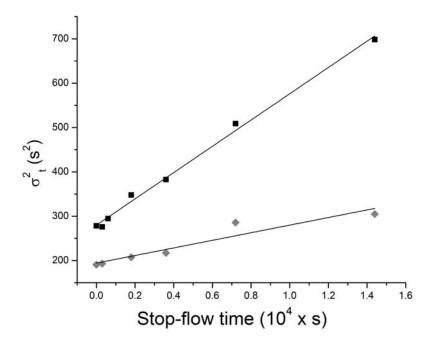
$$\sigma_z^2 = 2\ D_{eff}\ t_R \tag{3.16}$$

where $D_{eff}$ is the effective diffusion coefficient of the solute in the column and $t_R$ its retention time. $\sigma_z$ is related to the standard deviation of the band measured in units of time, $\sigma_t$, by the following formula:

$$\sigma_z = \sigma_t \times u \qquad (3.17)$$

where $u$ is the chromatographic velocity of the peak of interest upon elution. In terms of variances, then:

$$\sigma_z^2 = \sigma_t^2 \times u^2 \qquad (3.18)$$



**Figure 3.4**: Total variance, $\sigma_t^2$, plotted versus stop-flow time, $\Delta t_{off}$, for Ala-Val (diamonds) and (Ala)$_5$ (squares). The chromatographic velocities when the flow was on were $2.0 \times 10^{-4}$ and $2.9 \times 10^{-4}$ ms$^{-1}$ for Ala-Val and (Ala)$_5$, respectively. Linear fitting equations: $y = 151.6x + 272.9$, $R^2 = 0.9924$ (Ala-Val); $y = 78.9x + 196.9$, $R^2 = 0.9924$ ((Ala)$_5$).

When applying a stop-flow time, $\Delta t_{off}$, the following relationship is obtained:

$$t_R = t_{R,chrom} + \Delta t_{off} \qquad (3.19)$$

where $t_{R,chrom}$ is the analyte retention time in absence of stop-flow. By combining Eqs. 3.16, 3.18 and 3.19:

$$\sigma_t^2 = \sigma_{t,chrom}^2 + 2D_{eff}\,\frac{\Delta t_{off}}{u^2} \qquad\qquad (3.20)$$

where $\sigma_{t,chrom}^2$ is the total variance due to "normal" chromatographic effects and $2D_{eff} \times \Delta t_{off}/u^2$ is the contribution to the total variance due to stop-flow.

In Fig. 3.4, the plot of $\sigma_t^2$ *vs* $\Delta t_{off}$ is shown. From this figure it can be seen that a linear relationship is found to fit data quite well for both peptides and that the contribution to band broadening due to longitudinal diffusion increases more rapidly for Ala-Val, the lower MW peptide, than for $(Ala)_5$. $D_{eff}$ can then be easily calculated from the slope of the curve in Fig. 3.4. For Ala-Val a $D_{eff}$ of $3.0 \times 10^{-10}$ m$^2$s$^{-1}$ was obtained. The *B*-value hence is $6.0 \times 10^{-10}$ m$^2$s$^{-1}$.

### 3.4.2 Deriving typical values of $^1u$, $^1L$ and $^1H$

A typical $^2$D chromatogram from our system is shown in Figure 3.5. The analysis time for each sample in the $^2$D was approximately 600 s. The peaks were approximately 10 s wide (see Fig. 3.5). Subtracting the column dead and equilibration time, the usable elution time window in each RPLC chromatogram was approximately 300 s. By dividing this by the average peak width, a $^2n_c$ of 30 is obtained. If a $n_{c,tot}$ of 300 is needed, $^1n_c$ must then be 10. The required plate count in the $^1$D for that peak capacity, $^1N$, will be 2700. The required chromatographic velocity for the $^1$D then can be obtained from Eq. 3.12. The resulting value is $7.7 \times 10^{-6}$ ms$^{-1}$. This corresponds to a flow rate of approximately 0.01 mLmin$^{-1}$. $^1H$ and $^1L$ now can be calculated from Eq. 3.10 and Eq. 3.4. They were found to be $9.4 \times 10^{-5}$ m and 280 mm, respectively. Once more, every other $^1$D column length and linear velocity results in non-optimal operating conditions where the two requirements of a given desired total peak capacity and the requirement of four $^2$D runs over a $^1$D peak cannot be met simultaneously.
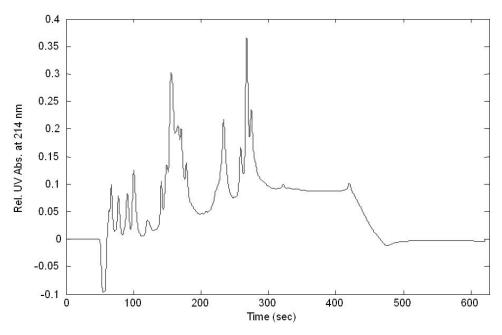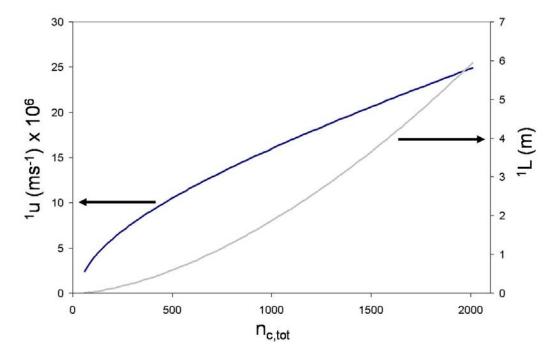
**Figure 3.5**: Single RPLC chromatogram (Fraction 27, extracted between 295.42 and 305.87 min).



**Figure 3.6**: Theoretical curves showing the chromatographic velocity in the $^1$D column, $^1u$, and the column length in the $^1$D column, $^1L$, as a function of the total desired peak capacity, $n_{c,tot}$.

Using the theory derived here and using the input parameters determined experimentally, also other scenarios can be calculated. Figure 3.6 shows the required column length and linear velocity as a function of the desired total peak capacity ($^2n_c$ is 30). Fig. 3.6 clearly shows that both $^1L$ and $^1u$ increase with the total peak capacity, $n_{c,tot}$,

and, therefore, with $^1n_c$. The conclusion that a longer column is needed to obtain a higher peak capacity might be not surprising, but the required length increase is more than linear because also a higher velocity is needed. While $^1L$ increases parabolically with $n_{c,tot}$, the relationship between $^1u$ and $n_{c,tot}$ can be obtained by substituting Eq. 3.3 in Eq. 3.12. In the limiting case of the $^1$D SEC column run at a very low linear velocity, however, the $B$-term dominates and, therefore, the $A$- and $C$-terms in Eq. 3.12 can be neglected. It can then be shown that $^1L$ is proportional to $n_{c,tot}^{3/2}$ and $^1u$ to $n_{c,tot}^{1/2}$ .

### 3.4.3 Establishing limiting conditions

As already noted, Eq. 3.11 does not have a physically meaningful solution if $^2t_a / \sqrt{^1N} \leq C$ . For the aqueous-SEC column used here, the $C$-value amounts to $8.6 \times 10^{-2}$ s. For a typical $^1$D plate number of 10,000, this means that, if the analysis time in the second-dimension gets below 9 s, there is no solution for Eq. 3.11. If, for the same column and the same $C$, $^2t_a$ equals 60 s, $^1N$ must be higher than $4.9 \times 10^5$ in order for Eq. 3.11 not to have solution. Clearly, and unfortunately we would say, under practical conditions one is hardly expected to encounter problems from this perspective.

### 3.4.4 Stop-flow vs Continuous Low-Flow

The calculations in Section 3.4.2 clearly show that the $^1$D column has to be operated at low to very low linear velocities. As previously discussed there are two ways to achieve this: continuous low-flow operation and stop-flow operation. Below, a comparison of these two modes in terms of band broadening will be presented. The values of the total variance for the two cases of continuous low-flow and stop-flow will be derived for Ala-Val, for a single interval of 10 minutes consisting of 9.50 minutes stop-flow and 0.50 minutes on-flow (see Fig. 3.1). Ala-Val was selected because this analyte presents a worst case scenario. It is small and hence has the highest axial dispersion coefficient.
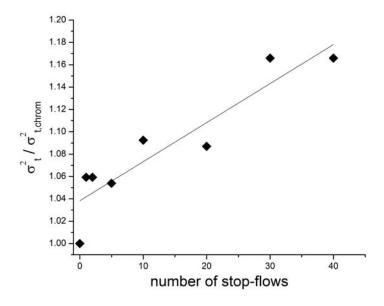
*Continuous low-flow.* In Section 3.4.2 the optimum linear velocity for the $^1$D column at a required total peak capacity of 300 is calculated to be $7.9 \times 10^{-6}$ ms$^{-1}$. The plate height $^1H$ then is $9.2 \times 10^{-5}$ m. From these values, $\sigma_{z,i}(cont)$ can be estimated, by means of Eq. 3.13, as $7.0 \times 10^{-4}$ m.

*Stop-flow.* In order to obtain the same average velocity in a stop-flow experiment where the flow is on only for 5% of the time, a twenty times higher linear velocity must be used during the "on-flow period". Substituting this velocity into Eq. 3.10 gives the plate height $^1H$ in the on-flow period. By using the previously determined $D_{eff}$ value, $\sigma_{z,i}(sf)$ was calculated to be $7.2 \times 10^{-4}$ m.

As the above exercise shows, the calculated band width for the two cases of continuous low-flow and stop-flow is basically identical. At first sight the above result might seem strange as it is commonly known that stop-flow periods in LC result in band-broadening due to longitudinal diffusion. To allow a fair comparison, however, stop-flow operation should be compared with continuous low-flow operation with an identical total retention time. If the elution time in intermittent high/low flow operation is identical to that in continuous low-flow operation, the total time for longitudinal diffusion is constant and hence the total effect is identical. In considering stop-flow operation in on-line LC × LC it is a common misconception to identify the stop-flow period as an additional source of band broadening, at least if the $^1D$ is operated at below optimum velocities, which will generally be the case in on-line LC × LC.

In order to see whether the repeated on/off switching could cause additional band broadening, a further experiment was performed. In short: (a) the sample is eluted for a certain time; (b) at $t = t_{stop}$ the pump is stopped; (c) after a time $\Delta t_{off}$ the pump is turned on again; (d) after a time $\Delta t_{on}$ (where $\Delta t_{on}$ is the time length in which the pump is turned on) the pump is switched off again; (e) steps (c) to (d) are repeated $n$ times; (f) the solute is finally eluted (with the flow-rate equal to that at the beginning). In order to minimize the contribution of longitudinal diffusion to the band width during the stop-flow period, $\Delta t_{off}$ was kept short (30 s). The results of this experiment are shown in Figure 3.7. From Fig. 3.7, it can be seen that the total variance in units of time, $\sigma_t^2$, increases slightly when the number of stop-flows is increased. Still, as this effect is quite small, it seems more logical to relate it to the longitudinal diffusion of the analyte inside the column during the stop-flow intervals rather than to the effect of switching the pump on and off. This is indeed confirmed by the experimental data: switching the pump off 20 times results in a peak width at half height, $w_{1/2}$, of 39.2 s, comparable with the value of 39.1 s obtained

when switching the pump off only once but then for 10 minutes. In conclusion, Eq. 3.20 was confirmed to properly describe band spreading when stop-flow is used.



**Figure 3.7**: Effect of number of stop-flows on band broadening. Ratio between total variance, $\sigma_t^2$, and total variance in absence of stop-flow, $\sigma_{t,chrom}^2$, plotted versus number of stop-flows for Ala-Val. Clearly, for $\Delta t_{off} = 0$, $\sigma_t^2 = \sigma_{t,chrom}^2$.
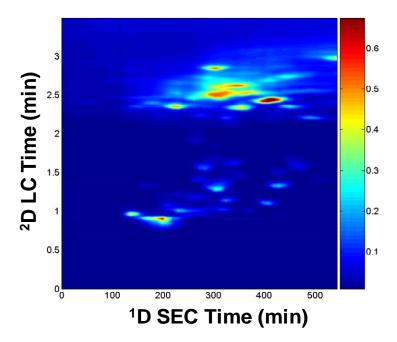
### 3.4.5 Instrument design criteria

In addition to operational parameters such as column length and flow rate, also practical issues such as the method of interfacing will affect the final result in a 2D separation of peptides. Two factors complicate the development of systems for on-line SEC × LC of peptides. Firstly, peptides are very prone to give significant retention time shifts depending on column quality and exact gradient composition. Secondly, especially the non-polar small peptides present in food protein hydrolysates are very susceptible to adsorption in all types of interfaces, storage loops, tubing etc. Knowing these problems we designed a comprehensive 2D-LC system around one $^2$D column and a minimum of interfaces between the two columns (see Fig. 3.2). A clear advantage of stop-flow operation in this respect is that no storage loops are needed. A simple valve suffices to transfer fractions from the first- to the second-dimension.
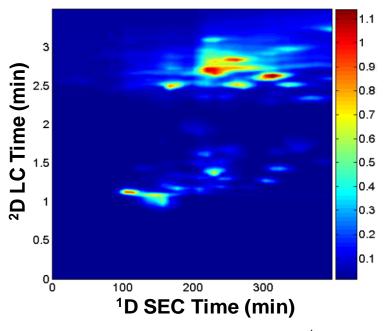
*3.4.6 Applications*

The theory approach derived in Section 3.2 was exploited to obtain the $^1$D parameters to be used in the on-line SEC × LC analysis. The result of an on-line SEC × LC experiment performed at the calculated optimum settings and delivering a total peak capacity of 300 is shown in Fig. 3.8. Fig. 3.8 clearly shows that adding a second column - the $^1$D column in the newly built on-line SEC × LC system – results in a resolving power comparable with that of the most successful one-dimensional separation systems published in the literature [24, 25]. The two requirements of a desired total peak capacity of 300 and of four $^2$D runs over a $^1$D peak, however, result in an unpractical analysis time. The total analysis time exceeds 500 minutes. This is the price to pay for the higher resolving power. Shorter analysis times are only possible if the analysis time of the $^2$D can be reduced or if a lower total peak capacity is accepted. Operating the $^1$D column at another flow rate is not an option to reduce the analysis time. Under such conditions the two requirements for truly comprehensive operation will not be met simultaneously.

A second experiment was performed by running the system in such a way that the number of $^2$D runs over each $^1$D peak was decreased from four to three. In order to do that, the $^1$D column flow rate was increased to 0.50 mLmin$^{-1}$ while keeping the actual transfer time constant at 30 s. Because of the increased transferred volume, the total number of fractions transferred from the first- to the second-dimension was decreased. Therefore, under these conditions, the total analysis time could be reduced to approximately 400 min. The 3D plot for this separation is shown in Figure 3.9.

The effect of sampling each peak from the $^1$D just three times is presented in Figure 3.10 in which a detail from Fig. 3.8 and Fig. 3.9 is compared. From Fig. 3.10 it is evident that the resolving power at this lower sampling frequency is sensitively decreased. Once more, it is important to emphasize that the choice of the sampling frequency of first-dimension peaks plays a very important role in the optimization of LC × LC separations. Neglecting this aspect can lead to dramatic decreases in overall resolving power. This aspect is discussed in more detail in Chapter 2.
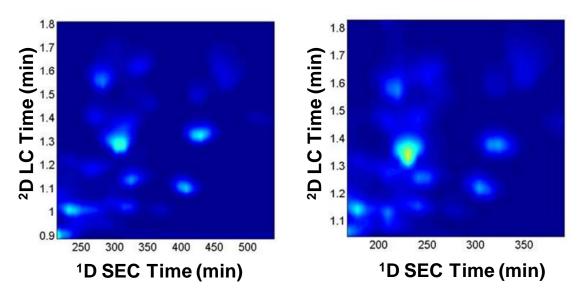
**Figure 3.8**: SEC × LC contour plot of BioZate3 at the optimal ${}^1$D conditions. $F = 0.37$ mLmin${}^{-1}$, operated in stop-flow mode (flow on for 0.5 min followed by flow off for 9.5 min). For other settings see Experimental Section.



**Figure 3.9**: SEC × LC contour plot of BioZate3 at non-optimal ${}^1$D conditions. $F = 0.50$ mLmin${}^{-1}$, operated in stop-flow mode (flow on for 0.5 min followed by flow off for 9.5 min). For other settings see Experimental Section.

An advantage in transferring larger volumes from the first- to the second-dimension column is that the dilution factor will be decreased, resulting in a more intense signal. Refocusing of the larger band on the $^2$D column was not an issue. The peptides are strongly retained at the initial gradient settings.

When running the $^1$D column, some undesired adsorption phenomena could not be avoided and, therefore, not all peaks eluted in the size exclusion mode (for a typical SEC run, see Fig. 3.3). In order not to make the total analysis time even longer these peaks were not sampled. The addition of an organic modifier did not really prevent adsorption.



**Figure 3.10**: Detail of Fig. 3.8 (left) and Fig. 3.9 (right) showing the influence of operating at non-optimum conditions.

## 3.5 Conclusions

In this chapter, a method for the selection of the operational parameters for the $^1$D of on-line LC × LC systems was derived. It was shown that, in order to simultaneously meet the two requirements of a certain desired total peak capacity and of four $^2$D runs over a $^1$D peak, only one set of conditions (column length, linear velocity) can be adopted for the $^1$D.

A system for on-line SEC × LC was designed and constructed. The derived theory was used for finding the optimal $^1$D conditions, for a situation where the $^2$D separation was already fixed. The on-line SEC × LC system, differently from what appeared in literature

so far, was run in stop-flow mode. In contrast to the common conception, stop-flow operation does not result in additional band broadening. Stop-flow interfacing is attractive as it greatly facilitates instrument design. The resulting system was applied to the analysis of complex mixtures of peptides derived from whey proteins.

## 3.6 References

[1] Bushey, M. M., Jorgenson, J. W., *Anal. Chem.* 1990, 62, 161-167.

[2] Banks, J. F., Gulcicek, E. E., *Anal. Chem.* 1997, 69, 3973-3978.

[3] Guzzetta, A. W., Hancock, W. S. in Hancock, W. S. (Editor), *New methods in peptide mapping for the Characterization of Proteins*, CRC Press, New York, 1996, Chapter 7, p. 181.

[4] Stults, J. T., Gillece-Castro, B. L.. Henzel, W. J., Bourell, J. H., O'Connell, K. L., Nuwaysir, L. M., in Hancock, W. S. (Editor), *New methods in peptide mapping for the Characterization of Proteins*, CRC Press, New York, 1996, Chapter 5, p. 119.

[5] Schoenmakers, P. J., Marriott, P., Beens, J., *LC-GC Eur.* 2003, 16, 335-339.

[6] Opiteck, G. J., Jorgenson, J. W., Anderegg, R. J., *Anal. Chem.* 1997, 69, 2283-2291.

[7] Holland, L. A., Jorgenson, J. W., *Anal Chem.* 1995, 67, 3275-3283.

[8] Wagner, K., Miliotis, T., Marko-Varga, G., Bischoff, R., Unger, K. K., *Anal. Chem.* 2002, 74, 809-820.

[9] Stoll, D. R., Carr, P. W. *J. Am. Chem. Soc.* 2005, 127, 5034-5035.

[10] Lemieux, L., Piot, J.-M., Guillochon, D., Amiot, J., *Chromatographia* 1991, 32, 499-504.

[11] Stromqvist, M., *J. Chromatogr. A* 1994, 667, 304-310.

[12] Vensel, W. H., Fujita, V. S., Tarr, G. E., Margoliash, E., Kaiser, H., *J. Chromatogr.* 1983, 266, 491-500.

[13] van der Horst, A., Schoenmakers, P. J., *J. Chromatogr. A.* 2003, 1000, 693-709.

[14] Dugo, P., Favoino, O., Luppino, R., Dugo, G. , Mondello, L., *Anal. Chem.* 2004, 76, 2525-2530.

[15] Coulier, L., Kaal, E. R., Hankemeier, Th., *Pol. Degr. Stab.* 2006, 91, 271-279.

[16] Giddings, C. J., *Anal. Chem.* 1984, 56, 1258A-1270A.

[17] Slonecker, P. J., Li, X., Ridgway, T. H., Dorsey, J. G. *Anal. Chem.* 1996, 68, 682-689.

[18] Gilar, M., Olivova, P., Daly, A. E., Gebler, J. C., *Anal. Chem.* 2005, 77, 6426-6434.

[19] Schoenmakers, P. J., Vivó-Truyols, G., Decrop, W. M. C., *J. Chromatogr. A* 2006, 1120, 282-290.

[20] Vivó-Truyols, G., van der Wal, S., Schoenmakers, P. J., *Anal. Chem.* 2010, 82, 8525-8536.

[21] Murphy, R. E., Schure, M. R., Foley, J. P., *Anal. Chem.* 1998, 70, 1585-1594.

[22] Giddings, ] C. J., *Anal. Chem.* 1967, 39, 1027-1028.

[23] Knox, J. H., Scott, H. P., *J. Chromatogr.* 1983, 282, 297-313.

[24] Luo, Q., Shen, Y., Hixson, K. K., Zhao, R., Yang, F., Moore, R. J., Mottaz, H. M., Smith, R. D. *Anal. Chem.* 2005, 77, 5028-5035.

[25] Wang, X., Barber, W. E., Carr, P. W., *J. Chromatogr. A* 2006, 1107, 139-151.